

Role of interfacial roughness on bias-dependent magnetoresistance and transport properties in magnetic tunnel junctions

J. C. A. Huang^{a)} and C. Y. Hsu

Department of Physics, National Cheng Kung University, Tainan, Taiwan, Republic of China, Department of Applied Physics, National University of Kaohsiung, Kaohsiung, Taiwan, Republic of China, and Taiwan Spin Research Center, National Chung Cheng University, Chiayi, Taiwan, Republic of China

Y. F. Liao, M. Z. Lin, and C. H. Lee

Department of Engineering and System Science, National Tsing-Hua University, Hsinchu, Taiwan, Republic of China

(Received 19 July 2005; accepted 5 October 2005; published online 17 November 2005)

The effects of metal-insulator interfacial roughness, modulated by Ar^+ irradiation, on bias dependence of tunnel magnetoresistance (TMR) and electrical transport of $\text{CoFe-AIO}_x\text{-CoFe}$ magnetic tunnel junctions (MTJs) have been studied. Reduction of TMR ratio and asymmetric TMR falloff curves as a function of dc bias have been observed for Ar^+ -irradiated MTJs. The results are analyzed by x-ray reflectivity together with complex impedance techniques, indicating interfacial roughness which likely results in a proportional rising trap state density (TSD). Increasing TSD for Ar^+ -irradiated MTJs increases an unpolarized current which decreases TMR ratio. The asymmetric TMR falloff curves are attributed to the different TSDs of bottom and top CoFe-AIO_x interfaces in tunneling process. © 2005 American Institute of Physics. [DOI: 10.1063/1.2132096]

I. INTRODUCTION

Giant tunnel magnetoresistance (TMR) effect in magnetic tunnel junctions (MTJs) has been extensively studied because of potential applications in nonvolatile magnetoresistive random access memory, high-density magnetic recording, and advanced magnetic devices in the next generation.^{1,2} From the application viewpoint, one of the key issues on how MTJs can be used is the dc bias voltage dependence of TMR. The dramatic decrease in TMR ratio with increasing bias voltage (or so-called TMR falloff curves) has been experimentally and theoretically investigated and was attributed to the possible origins of spin excitation localized at metal-insulator (M-I) interfaces, the impurity-assisted tunneling in tunnel barrier, and bias-dependent density of states of ferromagnetic electrodes.³⁻⁵ Asymmetric TMR falloff curves have been observed in MTJs with formation of improper-oxidized and composite tunnel barriers, Heusler alloys ferromagnetic electrodes, and MTJs subjected to annealing process.⁵⁻⁸ The asymmetric TMR falloff curves generally were believed to be due to different interfacial conditions of top and bottom M-I interfaces in MTJs.^{5,6} However, the origin of this phenomenon remains unclear so far.

We would like to understand the impact of interfacial roughness on TMR falloff curves and transport properties of MTJs. First, precise control of oxidation process for tunnel barrier has been achieved to exclude improper oxidation effects on the TMR falloff curves and transport properties of MTJs. Based on the interfacial modulation technique,⁹ we design a study to only modulate the M-I interfacial roughness under different Ar^+ irradiation times (t_{Ar}). X-ray reflectivity together with complex capacitance (CC) and bias-dependent complex impedance (CI) techniques¹⁰ are utilized

to probe the M-I interfacial roughness and barrier quality. The mechanisms of the observed reduction of TMR ratio, asymmetric TMR falloff curves, and variation of ac transport properties of MTJs are investigated.

II. EXPERIMENTAL DETAILS

MTJs of $\text{CoFe}(25\text{ nm})/\text{AlO}_x(\sim 3\text{ nm})/\text{CoFe}(10\text{ nm})$ were prepared on glass substrates by a dual ion-beam sputter system with a base pressure of 5×10^{-7} Torr. The Ar^+ irradiation was processed with a fixed acceleration voltage of 100 V on the bottom CoFe electrodes before the initial Al layer deposition. The t_{Ar} was varied from 0 to 300 s. The AlO_x layer was fabricated by exposing the Al layer under O_2/Ar ion-beam irradiation with the proper-oxidized condition.¹⁰ X-ray reflectivity was performed at the wiggler BL17A beamline of the National Synchrotron Radiation Research Center in Hsinchu, Taiwan.

III. RESULTS AND DISCUSSION

Figure 1(a) shows the selected TMR curves of $\text{CoFe-AIO}_x\text{-CoFe}$ MTJs with $t_{\text{Ar}}=0, 75$, and 300 s. Indeed we observe TMR ratio gradually decreases from 7.5% to 1.3% when t_{Ar} increased from 0 to 300 s. The decrease of TMR ratio, induced by Ar^+ irradiation, generally can be correlated to the change of barrier quality and/or the interfacial roughness. The CC spectroscopy has been demonstrated to be a convenient tool in probing the barrier quality of MTJs.¹⁰ The CC spectra of the 0, 75, and 300 s Ar^+ -irradiated MTJs display a concave at intersection of the rising tail and the arc, as shown in Fig. 1(b). This specific feature indicates that all the tunnel barriers situate in the optimized oxidation condition, i.e., the improper oxidation possibility on decreasing TMR ratio of the MTJs can be excluded. Therefore, the de-

^{a)}Electronic mail: jcahuang@mail.ncku.edu.tw

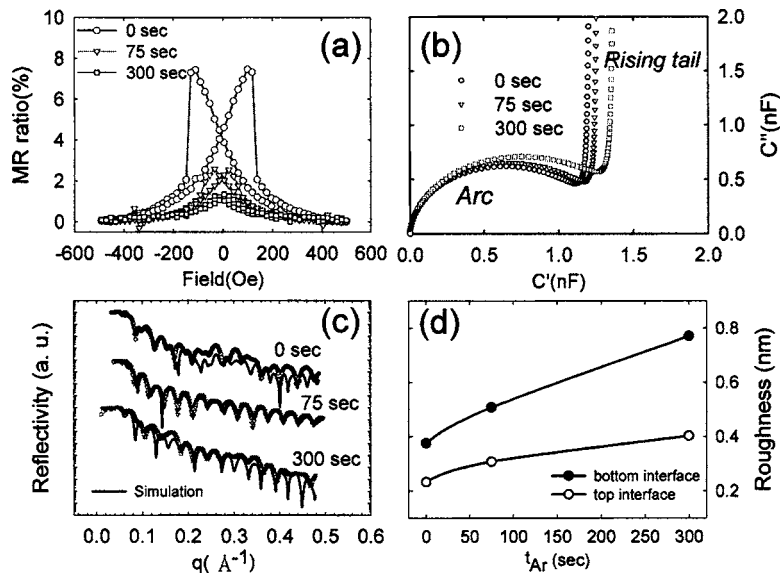


FIG. 1. (a) The TMR ratio, (b) complex capacitance spectra, (c) x-ray reflectivity with symbols for experimental data and curves for simulation results, and (d) fitting interfacial roughness of top and bottom M-I interfaces from x-ray reflectivity for Ar⁺-irradiated CoFe–AlO_x–CoFe MTJs with irradiation time t_{Ar} =0, 75, and 300 s.

crease of TMR ratio is solely due to the variation of the M-I interfacial roughness. To characterize the interfacial roughness of Ar⁺-irradiated MTJs, x-ray reflectivity spectra of the 0, 75, and 300 s Ar⁺-irradiated MTJs are presented in Fig. 1(c). For increasing t_{Ar} , the x-ray reflectivity peaks broaden and shift toward higher q values. The x-ray reflectivity data are further simulated and the fitting curves show good agreement with the experimental results, as illustrated in Fig. 1(c). The analyzing results of x-ray reflectivity, as shown in Fig. 1(d), indicate that the roughness profiles for the bottom and top M-I interfaces all increase with rising t_{Ar} . However, the roughness of the bottom M-I interface is larger than the top one and their difference enhances with increasing t_{Ar} . As induced by Ar⁺ irradiation, the increasing M-I interfacial roughness is responsible for the reduction of TMR ratio.

The dc bias dependence of TMR ratio is critical to optimize the performance of MTJs in application. The normalized TMR falloff curves of 0, 75, and 300 s Ar⁺-irradiated MTJs are demonstrated in Fig. 2. Here the normalized TMR ratio is defined as the normalization of $(R_0 - R_s)/R_0$, where R_0 and R_s are, respectively, the junction resistance of zero and saturated field. The normalized TMR falloff curves show two specific features. First, symmetric normalized TMR falloff curves have been observed for $t_{Ar}=0$ MTJs, but they

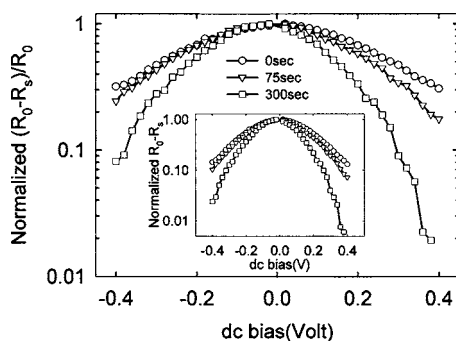


FIG. 2. Normalized TMR falloff curves as a function of V_{dc} ranged from -400 to 400 mV for Ar⁺-irradiated CoFe–AlO_x–CoFe MTJs with irradiation time t_{Ar} =0, 75, and 300 s. The inset indicates the patterns of normalized $R_0 - R_s$ vs V_{dc} .

become apparently asymmetric with increasing t_{Ar} . Secondly, the normalized TMR falloff curves for $t_{Ar}=0$ MTJs demonstrate a slow decrease with increasing dc bias (V_{dc}), in contrast with a faster decrease for increasing t_{Ar} . To explain the above phenomena, advanced analyses by bias-dependent CI spectra are further employed to probe the M-I interfacial transport properties for the Ar⁺-irradiated MTJs. In the measurement of bias-dependent CI spectra, a suitable choice of V_{dc} amplitude is essential to probe the interfacial conditions. The dc four-point-probe (4p) current-voltage (I - V) curves provide useful information for the choice of bias amplitude. Figure 3(a) displays the dc 4p I - V curves of 0, 75, and 300 s Ar⁺-irradiated MTJs. The I - V curves of the 75 and 300 s Ar⁺-irradiated MTJs almost overlap in low-bias-voltage region, but these two I - V curves become distinguishable when V_{dc} exceeds about 100 mV. Therefore, we apply an additional V_{dc} of 400 mV [typical for magnetic random access memory (MRAM) operation] in the measurement of CI spectra. Based on the above design, the bias-dependent CI spectra can be used to probe the variation of the top and bottom M-I interfacial conditions perturbed by Ar⁺ irradiation on the bottom electrode.

Figure 3(b) demonstrates the bias-dependent CI spectra (at 400 mV dc bias from bottom to top electrodes) in type of log-log Nyquist plots. The bias-dependent CI spectra can be analyzed by equivalent circuit method, including the contributions for CoFe–AlO_x interfaces (R_i and C_i), bulk AlO_x layer (R_b and C_b), and lead of cross patterns (R_l). The fitting curves in Fig. 3(b) demonstrate great agreement with experimental results. Among these parameters, R_i and C_i are the dominant factors related to the M-I interfacial transport properties discussed below. First, we observe that the interfacial capacitance (C_i) increases with rising t_{Ar} , as shown in Fig. 3(c). It is noted that C_i can be influenced by the charge redistribution inside the tunnel barrier near the interface or by variation of interfacial traps.¹¹ The former process, similar to the formation of p - n junctions, occurs only at a larger length scale (>100 nm), thus, the possibility can be obviated. The latter process enhances the C_i in proportion to the

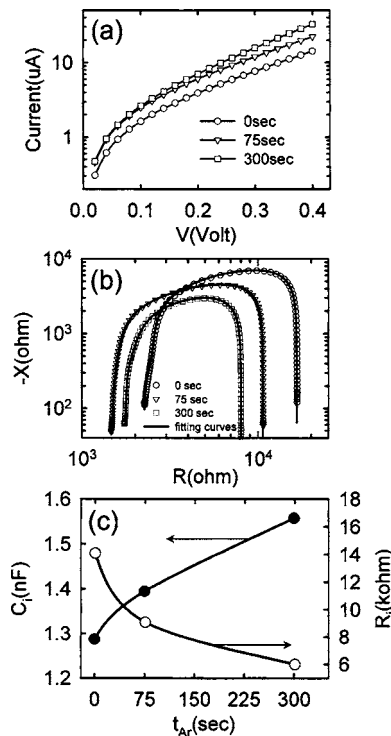


FIG. 3. (a) The four-point-probe current-voltage curves, (b) bias-dependent complex capacitance spectra in type of Nyquist plots (symbols) in log-log scale and fitting curves (solid curves), (c) fitting interfacial capacitance C_i , and (d) fitting interfacial resistance R_i for CoFe–AlO_x–CoFe MTJs with irradiation time $t_{Ar}=0, 75$, and 300 s.

trap state density (TSD) or the lifetime an electron spends on the trap states near the M-I interface. The enhancement in C_i likely indicates that the Ar⁺ irradiation creates more trap states at the M-I interfaces. Second, these trap states are likely formed by the hybridization of conduction carriers and defects at M-I interfaces. When carriers are injected from the bottom ferromagnetic (FM) electrode across the M-I interface to the insulating layer, these trap states act as conducting channels. Thus, the increase in TSD with rising t_{Ar} causes a decrease in R_i , as shown in Fig. 3(c), as a consequence of increasing conducting channels. Furthermore, the increase in TSD suggests that more defects are created at the M-I interface due to increasing of the interfacial roughness by Ar⁺ irradiation, consistent with the results of x-ray reflectivity. It is here noted that similar results of bias-dependent CI spectra have also been observed when MTJs are biased from the top to the bottom electrodes.

Finally, we attempt to clarify the underlying mechanism for the asymmetric TMR falloff curves. The asymmetric TMR falloff curves of the 75 and 300 s Ar⁺-irradiated MTJs can be due to the variation of junction resistance (R_0), $R_0 - R_s$, or their mixed contributions. We notice that the junction resistance of all MTJs decrease with increasing V_{dc} , but these curves (not shown here) are in marked difference with the patterns of Fig. 2. The possibility of junction resistance variation causing the asymmetric properties can be eliminated. We also plot the normalized $R_0 - R_s$ vs V_{dc} . As shown

in the inset of Fig. 2, the curves are almost the same as the normalized TMR falloff curves. The asymmetric properties hence are due to the spin-dependent contribution as further interpreted in the following. MTJs with increasing top and bottom interfacial roughnesses, shown in Fig. 1(d), show increasing TSD at bottom and top interfaces. When spin-polarized (SP) carriers are injected from the bottom FM electrodes (positive bias region), the SP carriers first encounter the bottom interface with a higher TSD. These trap states behave as unpolarized channels, thus, the SP carriers decrease more dramatically during tunneling through the bottom M-I interface. On the contrary, SP carriers injected from top FM electrodes (negative bias region) first encounter the top interface with a relatively lower TSD, i.e., more SP carriers tunnel through the top M-I interface compared to the reverse bias process. When V_{dc} increases, the difference of spin-independent currents become apparent and lead to asymmetric TMR falloff curves in the positive and negative regions.

IV. CONCLUSIONS

In summary, asymmetric TMR falloff curves have been observed for Ar⁺-irradiated MTJs. CI and x-ray reflectivity techniques have been employed to characterize the Ar⁺-irradiated M-I interfaces. An interpretation, based on the distribution of TSD at M-I interfaces, has been proposed to disclose the underlying mechanism for the asymmetric TMR falloff curves. This work also demonstrates that the control of interfacial roughness can be utilized to modulate the transport properties of MTJs.

ACKNOWLEDGMENTS

The authors would like to thank Professor Y. H. Lee for the kind assistance of using the impedance analyzer. This work has been support by the National Science Council of the ROC under Grant No. NSC 94-2112-M-006-003, Taiwan Spin Research Center of the National Chun Cheng University under Grant No. 93-EC-17-A-01-S1-026, and National Synchrotron Radiation Research Center under Project No. 2004-3-032-1.

¹G. A. Prinz, *Science* **282**, 1660 (1998).

²S. S. P. Parkin, C. Kaiser, A. Panchula, P. M. Rice, B. Hughes, M. Samant, and S. H. Yang, *Nat. Mater.* **3**, 862 (2004).

³S. Zhang, P. M. Levy, A. C. Marley, and S. S. P. Parkin, *Phys. Rev. Lett.* **79**, 3744 (1997).

⁴J. Zhang and R. M. White, *J. Appl. Phys.* **83**, 6512 (1998).

⁵X. H. Xiang, T. Zhu, J. Du, G. Landry, and J. Q. Xiao, *Phys. Rev. B* **66**, 174407 (2002).

⁶L. Le Brizoual, P. Alont, M. Hehn, F. Montaigne, M. Alont, A. Schuhl, and E. Snoeck, *Appl. Phys. Lett.* **86**, 112505 (2005).

⁷J. Schmalhorst, S. Kämmerer, G. Reiss, and A. Hütten, *Appl. Phys. Lett.* **86**, 052501 (2005).

⁸S.-J. Ahn, T. Kato, H. Kubota, Y. Ando, and T. Miyazaki, *Appl. Phys. Lett.* **86**, 102506 (2005).

⁹Y. Miyamoto, K. Machida, N. Hayashi, T. Tamaki, and H. Okuda, *J. Appl. Phys.* **89**, 6647 (2001).

¹⁰J. C. A. Huang and C. Y. Hsu, *Appl. Phys. Lett.* **85**, 5947 (2004).

¹¹G. Landry, Y. Dong, J. Du, X. Xiang, and J. Q. Xiao, *Appl. Phys. Lett.* **78**, 501 (2001).